

Importance of dynamic lattice effects for crystal field excitations in quantum spin ice candidate $\text{Pr}_2\text{Zr}_2\text{O}_7$.

Yuanyuan Xu,¹ Huiyuan Man,^{1,2} Nan Tang,^{1,2} Santu Baidya,³ Honbin Zhang,³ Satoru Nakatsuji,^{2,4,5,6,7} David Vanderbilt,³ and Natalia Drichko¹

¹*Institute for Quantum Matter and Department of Physics and Astronomy, Johns Hopkins University, Baltimore, Maryland 21218, USA*

²*Institute for Solid State Physics, University of Tokyo, Kashiwa, Chiba 277-8581, Japan*

³*Department of Physics and Astronomy, Rutgers University*

⁴*CREST, Japan Science and Technology Agency, Kawaguchi, Saitama 332-0012, Japan*

⁵*Institute for Quantum Matter and Department of Physics and Astronomy, Johns Hopkins University, Baltimore, MD 21218, USA*

⁶*Department of Physics, University of Tokyo, Bunkyo-ku, Tokyo 113-0033, Japan*

⁷*Trans-scale Quantum Science Institute, University of Tokyo, Bunkyo-ku, Tokyo 113-0033, Japan*

(Dated: July 28, 2021)

$\text{Pr}_2\text{Zr}_2\text{O}_7$ is a pyrochlore quantum spin-ice candidate. Using Raman scattering spectroscopy we probe crystal electric field excitations of Pr^{3+} , and demonstrate the importance of their interactions with the lattice. We identify a vibronic interaction with a phonon that leads to a splitting of a doublet crystal field excitation at around 55 meV. We also probe a splitting of the non-Kramers ground state doublet of Pr^{3+} by observing a double line of the excitations to the first excited singlet state $E_g^0 \rightarrow A_{1g}$. We show that the splitting has a strong temperature dependence, with the doublet structure most prominent between 50 K and 100 K, and the weight of one of the components strongly decreases on cooling. We suggest a static or dynamic deviation of Pr^{3+} from the position in the ideal crystal structure can be the origin of the effect, with the deviation strongly decreasing at low temperatures.

I. INTRODUCTION

Much of condensed matter research is currently focused on a search for an experimental realization of a quantum spin liquid (QSL) state. This is a magnetic state, where spins do not order despite strong interactions, but nevertheless their behavior is determined by strong non-local correlations [1, 2]. It is already understood that this state can be brought about by a presence of a strong geometric frustration or competing interactions. In addition, many candidate systems show some levels of structural disorder. It is still a question, if the disorder prevents quantum phenomena and mocks them experimentally, or it can be a factor leading to a QSL state [2]. Another important question is how to experimentally distinguish the effects of structural disorder from the effects produced by dynamics of the lattice. In this work on a quantum spin ice candidate $\text{Pr}_2\text{Zr}_2\text{O}_7$ [3, 4] we show that Raman scattering spectroscopy is able to separate dynamic effects from the effects of structural disorder. In the case of $\text{Pr}_2\text{Zr}_2\text{O}_7$ our study finds evidence of dynamic lattice effects and shows their importance for the magnetic state of this material.

$\text{Pr}_2\text{Zr}_2\text{O}_7$ is a pyrochlore material, where the crystal structure provides a three dimensional frustrated lattice. Pyrochlores are known to host classical spin ice [5–8] and quantum spin ice, where quantum fluctuations are no longer negligible [9, 10]. Magnetic properties of $\text{Pr}_2\text{Zr}_2\text{O}_7$ are defined by the magnetic moment of Pr^{3+} . In a crystal, 3H_4 level of $4f$ atomic orbitals of Pr^{3+} which carry $J = 4$ magnetic moment is split under the influence of the electric fields related to the local D_{3d} crystal sym-

metry [11, 12] into $2A_{1g} + A_{2g} + 3E_g$ multiplets. This splitting determines magnetic properties of the system. The ground state of the system is the E_g non-Kramers doublet. A non-Kramers doublet ground state makes the magnetic system sensitive to the lattice degree of freedom, since a small deviation from D_{3d} local symmetry can bring about a splitting of the ground state. This is the basis of suggestions that a local disorder is an important factor in the formation of a quantum spin ice ground state in $\text{Pr}_2\text{Zr}_2\text{O}_7$ [4, 13], as well as a possibility of studies of quantum spin ice by magnetostriction, which were applied to $\text{Pr}_2\text{Zr}_2\text{O}_7$ [14, 15].

The crystal electric field (CEF) description takes into account the lattice degrees of freedom as static, and decoupled from the electronic and magnetic degrees of freedom. This is not always a good approximation. For rare earth materials in particular, the presence of vibronic states, where phonons modulate crystal field levels, is possible, due to the overlapping energy ranges of these excitations. These interactions are not yet widely studied for rare earth pyrochlores, but the example of $\text{Tb}_2\text{Ti}_2\text{O}_7$, where vibronic coupling is so close to the ground state that it can affect its properties leading to spin liquid state, shows that this dynamic interactions cannot be neglected [16–18].

Here we present our new findings on the crystal field levels of Pr^{3+} in $\text{Pr}_2\text{Zr}_2\text{O}_7$ and their coupling to the lattice. High spectral resolution and symmetry selectivity of Raman scattering spectroscopy allows a new look at the importance of interactions with the lattice, going beyond simple crystal field splitting and the static approximation. We observe a splitting of the doubly-degenerate

crystal field levels with the nature of the splitting being different for the E_g levels of different energies. We demonstrate that the E_g level at 55 meV shows a splitting of 2.3 meV due to vibronic interactions missed in previous studies [3, 13, 19]. We also probe the E_g ground-state splitting and its evolution with temperature through the analysis of transitions to the lowest excited A_{1g} state. Our results suggest that the splitting is present prominently at temperatures around 100 K, and decreases on cooling. We discuss possible static and dynamic origins of this effect.

II. RESULTS

The temperature dependence of the Raman spectra of $\text{Pr}_2\text{Zr}_2\text{O}_7$ in the spectral range from 3.7 to 70 meV (30 to 565 cm^{-1}) at temperatures between 6 and 300 K is presented in Fig. 1. Raman spectra in the range up to 125 meV can be found in SI. In the Raman spectra of $\text{Pr}_2\text{Zr}_2\text{O}_7$ we observe two types of excitations: (i) Raman-active phonons; (ii) CEF excitations of Pr^{3+} . Phonons were identified by polarization-resolved Raman measurements on the (100) surface [20] and a comparison to the DFT phonons calculations, while CEF excitations were assigned based on neutron scattering results [3, 19, 21].

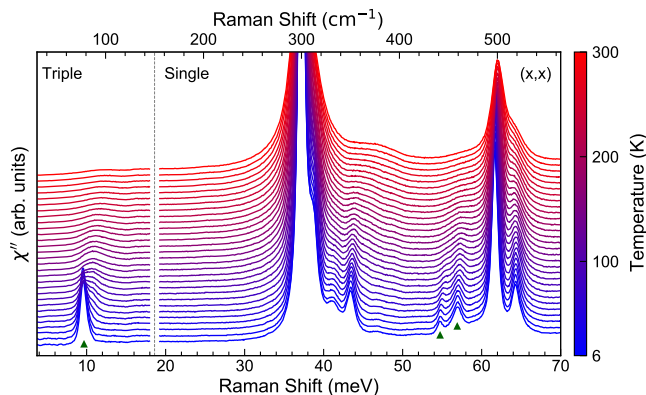


FIG. 1. Temperature dependence of the Raman scattering spectra of $\text{Pr}_2\text{Zr}_2\text{O}_7$ in the temperature range from 6 to 300 K in parallel polarization configuration (x, x) in the spectral region of the CEF. The spectra are shifted along y-axis for clarity. CEF excitations are marked by green triangles. The full measured spectral range up to 125 meV can be found in SI.

In this work we focus our attention on the CEF excitations in the spectra of $\text{Pr}_2\text{Zr}_2\text{O}_7$. Raman scattering can detect spectral lines of CEF excitations with much higher energy resolution (0.125 meV for our experiments) than that of the neutron scattering measurements, which can typically go down only to 1 meV in the high resolution measurements for low signals [22]. CEF excitations show a much stronger temperature dependence of the line width than phonons [23] (see Fig. 1), which allows

to observe most of them only at low temperatures.

TABLE I. Frequencies and widths of Pr^{3+} CEF levels obtained from the Raman scattering spectra at $T = 14$ K. For the A_{1g} excitation at 9.5 meV, the second component has below 10% of the spectral weight and is not included into the table. For the CEF excitations around 55 meV, v_1 and v_2 are magnetoelastically induced vibronic states which possess A_{1g} and E_g symmetry respectively.

Level	Frequency (meV)	Line width (meV)
A_{2g}	109.0	1.5
E_g	94.4	2.8
A_{1g}	82.1	1.5
v_2 (E_g)	57.1	1.2
v_1 (A_{1g})	54.8	0.6
A_{1g}	9.5	1.0

Energies of Pr^{3+} CEF excitations observed in the Raman spectra of $\text{Pr}_2\text{Zr}_2\text{O}_7$ (see Tab I) correspond well to that observed by neutron scattering [3, 19]. However, the line shapes measured with the higher spectral resolution provided a lot of new information. We present spectra of CEF at 14 K with phonons subtracted in Fig. 2(a). The main result is the Raman observation of splitting of the lower energy doublet levels, and the evidence for the different physical origins of the splitting of different excitations.

For higher energy CEF states, we observe a difference in line width between singlet and doublet excitations. At 14 K the spectral line corresponding to the excitation of the doublet E_g at 94 meV (762 cm^{-1}) shows a width of 2.8 meV, which is about two times larger than the width of the spectral lines of singlet A_{1g} and A_{2g} excitations (1.5 meV), see Table I, Fig 2(a).

The line of a doublet E_g at about 55 meV (460 cm^{-1}) is split into two components (v_1 and v_2) separated by 2.3 meV. The v_1 and v_2 components of the excitation show different symmetries, with the low-frequency component v_1 following the properties of $xx+yy$ basis functions (A_{1g} scattering channel), and the higher frequency one (v_2) following x^2-y^2 basis functions (E_g scattering channel), see Fig. 2a.

On increasing the temperature, the excitation lines broaden (for details see SI, Fig. 3). All the lines of the CEF excitations harden by about 1 meV on the increase of temperature.

At temperatures below about 20 K, the line of the CEF excitation to the lowest excited singlet A_{1g} level at 9.5 meV (Fig. 3) shows an asymmetric shape. It can be well described by two symmetric Gaussian-Lorentzian line shapes with the higher-frequency component of approximately 10 % of the total spectral weight of the excitation line. On the increase of the temperature, the spectral weight of the high-energy component increases, and the line develops into a well-defined doublet line with overlapping components at about 9.5 meV and 10.4 meV. The energy difference between the two components of the

doublet increases, and lines broaden on temperature increase (see Fig. 3(b)), until the components cannot be distinguished above 110 K. The doublet is identified most distinctly in the temperature range between 50 K and 100 K. The components of the doublet do not show any polarization dependence. The slight asymmetry is also present in the line shapes of the higher-frequencies A_{1g} CEF excitations, however, at all temperatures they are much broader than the energy difference between the two components of the excitation at 9.5 meV.

III. DISCUSSION

According to the average crystal structure [12], the $4f$ level of Pr^{3+} in $\text{Pr}_2\text{Zr}_2\text{O}_7$ is split by the crystal field of D_{3d} symmetry into $2A_{1g} + A_{2g} + 3E_g$ multiplets. In the Raman scattering spectra we observe excitations from the ground state doublet to all higher-energy components of this multiplet [3]. However, neither the symmetry-dependent splitting of the E_g level at 55 meV, nor the splitting of the A_{1g} level at 9.5 meV, can be understood within simple picture of the crystal field splitting according to D_{3d} symmetry.

A. Vibronic state for E_g excitation at 55 meV.

First, we discuss the origin of the splitting of the E_g level at 55 meV. The splitting between the resulting lines (2.3 meV) is larger than the splitting of the ground state doublet (1 meV), the latter estimated according to our data and to previously published neutron scattering data [4, 13].

The well-defined symmetry of the components shows that the splitting cannot be understood in terms of structural disorder leading to a relief of the double degeneracy of the level, contrary to the previous interpretation [13]. Such a symmetry-defined splitting can occur on mixing with another excitation of E symmetry, with $E \otimes E = E + A_1 + A_2$, where the resulting A_1 and E excitations will be observed in (x, y) and (x, x) scattering channels, as detected in our experiment. Thus the candidate excitation should have E symmetry and energy close to the 55 meV of the crystal field level. In $\text{Pr}_2\text{Zr}_2\text{O}_7$, similar to other rare-earth based crystals, a good candidate for such an excitation is a phonon.

Theory describing this vibronic process was first developed by P. Thalmeier et. al [24]. Typically, this mixing occurs when a CEF state and a phonon have the same symmetry and are close in frequency. The system can be described by the following Hamiltonian [24]

$$\mathcal{H} = \mathcal{H}_0 + \mathcal{H}_{\text{int}}, \quad (1)$$

with the non-interacting part:

$$\mathcal{H}_0 = \sum_{\alpha n} \epsilon_{\alpha} |\Gamma_{\alpha}^n\rangle \langle \Gamma_{\alpha}^n| + \hbar\omega_0 \sum_{\mu} (a_{\mu}^{\dagger} a_{\mu} + \frac{1}{2}) \quad (2)$$

and the interacting part

$$\mathcal{H}_{\text{int}} = -g_0 \sum_{\mu} U_{\mu} O_{\mu}. \quad (3)$$

The non-interacting part of the Hamiltonian (Eqn. 2) is composed of a CEF level $|\Gamma_{\alpha}\rangle$ of a rare earth ion with degeneracy index n and a coupled phonon with energy $\hbar\omega_0$. In the interacting part (Eqn. 3), $U_{\mu} = a_{\mu} + a_{\mu}^{\dagger}$ is the phonon displacement operator and O_{μ} is the quadrupolar operator transforming like the symmetry of the phonon [25, 26]. The magnetoelastic coupling constant is given by g_0 . Importantly, this process is not restricted to any particular part of the Brillouin zone.

In the case of $\text{Pr}_2\text{Zr}_2\text{O}_7$, we can identify the phonon which produces the vibronic state. The calculated phonon dispersion in the relevant energy range is presented in Fig 2(d). At the Γ -point of the BZ, the calculations are in good agreement with the experimentally determined frequencies of the Raman-active phonons [20], and both show an absence of a doubly-degenerate phonon in the region of 55 meV. However, mixing is possible at the other parts of the BZ, which also puts less restrictions on the phonon symmetry. A simple assumption is that the energy of an unperturbed E_g crystal field excitation would be found between the two split components at 56 meV, as marked with a dashed line in Fig. 2. There are two phonon candidates that are very close in energy to this CEF excitation in the X to W part of the BZ. The most probable phonon candidate is a phonon which is observed at 64.6 meV (63.5 meV is the calculated frequency) at the Γ point (T_{2g}). The calculated dispersion of this phonon is plotted as a red line in Fig. 2(d). The eigenvector involves the movement of O1 oxygens, which modulate the Pr^{3+} oxygen environment (see Fig. 2(e)). We observe this vibronic effect in the Raman spectra at Γ -point, because the CEF excitations do not show dispersion, and the splitting which results from interactions in a certain part of BZ, leads to the splitting of the CEF levels observed over the whole BZ [22].

Our high resolution measurements of CEF excitations allow us to refine the crystal field parameters [19] and obtain values of magneto-elastic coupling constants, as shown in detail in the SI.

Rare earth atoms show CEF excitations in the energy range of the lattice phonons in many materials, and the vibronic effect involving the CEF excitations can be relatively common [22, 24, 27], though not broadly studied. Among pyrochlore rare earth based compounds, vibronic states are found, for example, in $\text{Ho}_2\text{Ti}_2\text{O}_7$ [22] and $\text{Tb}_2\text{Ti}_2\text{O}_7$ [28]. The latter is an especially interesting case, because a mixing of the very-low lying first excited state with a phonon might be an origin of a spin liquid state in this material [10].

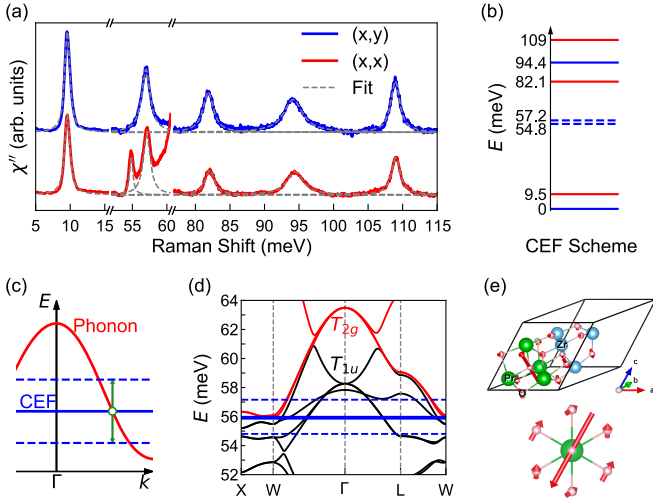


FIG. 2. (a) Raman spectra of CEF excitation of $\text{Pr}_2\text{Zr}_2\text{O}_7$ at 14 K. (b) A scheme of the CEF levels of Pr^{3+} in $\text{Pr}_2\text{Zr}_2\text{O}_7$. (c) Diagram of the vibronic coupling between the phonons and CEF states. (d) $\text{Pr}_2\text{Zr}_2\text{O}_7$ phonon dispersion obtained by DFT calculations. The energy range close to the vibronic features is shown. Dashed blue lines mark the experimentally observed CEF vibronic excitations. The vibronic coupling is expected to occur at the intersection point of the nonsplit CEF doublet (solid blue line) and the T_{2g} phonon branch (red curve). (e) Atomic displacements of the T_{2g} phonon mode. Upper panel: view of the unit cell. Lower panel: PrO_8 octahedron site viewed from the $[111]$ direction.

B. Probing the splitting of the ground state doublet.

The splitting of the A_{1g} CEF excitation at 9.5 meV has a very different character. The doublet line of this excitation does not show any polarization dependence. This symmetry consideration, together with an absence of the A_{1g} Γ -point phonons close to 9.5 meV, allows us to dismiss a vibronic state interpretation [29].

A splitting of the spectral line corresponding to the $E_g^0 \rightarrow A_{1g}$ excitation can reflect the doublet structure of the E_g^0 ground state level, as is schematically shown in Fig. 3. It can be understood easily by considering the relevant Raman intensity $\chi''(\omega)$ at each frequency ω_i :

$$\chi''(\omega_i, T) = B_{nk} \int_{-\infty}^{\infty} \rho(\omega', T) L(\omega_i - \omega', T) d\omega'. \quad (4)$$

Here the natural width of the A_{1g} singlet level is a Lorentzian function $L(\omega, T)$ determined by the lifetime of the level $\tau(T)$ [23], and $\rho(\omega, T)$ is the density of the E_g^0 level. B_{nk} a probability of $E_g \rightarrow A_{1g}$ transition.

We can use a deconvolution procedure for experimental Raman intensity $\chi(\omega)$ to obtain $\rho(\omega, T)$. The strong temperature dependence of the shape of the Raman excitation at around 9.5 meV reflects the change of $\rho(\omega, T)$ with temperature. We show $\rho(\omega, T)$ for a number of temperatures in Fig. 3(c). While the doublet structure

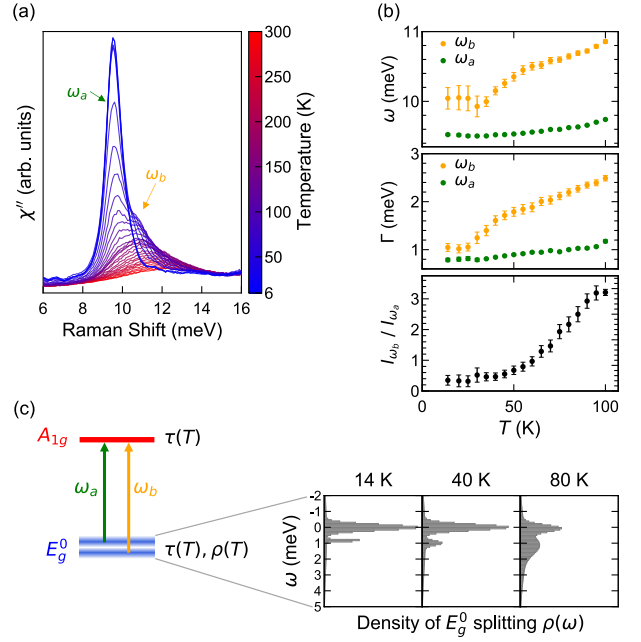


FIG. 3. (a) Temperature dependence of the Raman scattering spectra in the energy range of the lowest lying CEF excitation $E_g^0 \rightarrow A_{1g}$. (b) Upper panel: positions of the two components of the transition (ω_a and ω_b); middle panel: line widths of the two components of the excitations (ω_a and ω_b); lower panel: the ratio of the spectral weight of ω_b to ω_a . (c) The scheme of the excitation $E_g^0 \rightarrow A_{1g}$ illustrates that the shape of the electronic density distribution ρ of the E_g^0 level, such as splitting, can define the shape of the observed spectral excitation line. Histograms demonstrate the density of the ground state splitting $\rho(\omega)$ obtained by the deconvolution of the Raman scattering spectra at 14, 40, and 80 K.

is pronounced at temperatures between 100 and 40 K, the relative spectral weight of the high-frequency component decreases on cooling, reaching only 10% of the spectral weight of the lower-frequency component below 30 K. This temperature dependence is reversed to that expected due to the thermal population of the levels. $\rho(\omega_i, T)$ is approaching that of a single non-split E_g^0 level as the temperature is reduced. The non-smooth temperature dependence of the parameters of the E_g^0 components at around 30 K reflects the decrease of the low-energy weak component down to below 10% of the total weight. Interestingly, in this temperature range, a change of slope in magnetic susceptibility is observed (see SI) [3, 19]. At temperatures below about 30 K susceptibility is well-described by a non-split ground state CEF level only [19].

An observation of the E_g^0 doublet in Raman scattering was possible due the high spectral resolution, and presents a more complicated picture than a single band Gaussian distribution with width of 1 mW obtained from neutron scattering data [4, 13]. The latter was suggested to be a result of structural disorder [4], and in particularly random strain [13]. The presence of the two components

of E_g^0 separated by about 1 mW can explain a feature in the heat capacity of $\text{Pr}_2\text{Zr}_2\text{O}_7$ observed at about 10 K [3].

While random disorder cannot be the origin of the well-defined splitting, the split ground state doublet can be a result of a deviation of Pr^{3+} environment from D_{3d} . Such a deviation may be produced, for example, by a shift of the Pr^{3+} atom from the position in the average structure, and was suggested by B. Trump et. al [30]. The temperature dependence of the spectra corresponds to a decrease of a deviation of Pr^{3+} environment from D_{3d} on cooling, which can occur due to changes of structure on thermal contraction of the crystals.

Alternatively, the splitting can originate from a dynamic process. Such a process could be a phonon-like “jump” of Pr atom between a central position and an off-center potential minimum. Such a picture can explain the temperature dependence of both intensities and width of the E_g^0 components (Fig 3). On cooling, this dynamic process slows down or the phonon excitation gets de-populated, leading to the redistribution of spectral weight and narrowing of the levels that belong to the ground state E_g^0 doublet. If such a phonon mode exists, it would be a dipole-active excitation, observed in GHz regime.

IV. CONCLUSIONS

In this work we perform a high-resolution symmetry-resolved Raman scattering study of crystal field levels of Pr^{3+} in $\text{Pr}_2\text{Zr}_2\text{O}_7$, and show that dynamic interactions

with the lattice are the dominant reason for the splitting of the doublet crystal fields levels. We show that a 2.3 meV splitting of an E_g^0 crystal field level at 55 meV originates from a vibronic interaction with a phonon.

We detect a splitting of the ground state doublet by analyzing a transition to the first excited state $E_g^0 \rightarrow A_{1g}$. The splitting has a strong temperature dependence. We suggest possible interpretations in terms of static or dynamic shift of Pr^{3+} from the D_{3d} .

V. ACKNOWLEDGEMENTS

The authors are thankful to J. Gauget, C. Broholm, S. Bhattacharjee, T. McQueen, J-J. Wen, and O. Tchernyshev for useful discussions. This work was supported as part of the Institute for Quantum Matter, an Energy Frontier Research Center funded by the U.S. Department of Energy, Office of Science, Basic Energy Sciences under Award No. DE-SC0019331. This work in Japan is partially supported by CREST (Grant Number: JPMJCR18T3 and JPMJCR15Q5), by New Energy and Industrial Technology Development Organization (NEDO), by Grants-in-Aids for Scientific Research on Innovative Areas (Grant Number: 15H05882 and 15H05883) from the Ministry of Education, Culture, Sports, Science, and Technology of Japan, and by Grants-in-Aid for Scientific Research (Grant Number: 19H00650) and Program for Advancing Strategic International Networks to Accelerate the Circulation of Talented Researchers (Grant Number: R2604) from the Japanese Society for the Promotion of Science (JSPS).

-
- [1] C. Broholm, R. J. Cava, S. A. Kivelson, D. G. Nocera, M. R. Norman, and T. Senthil, *Science* **367**, 10.1126/science.aay0668 (2020).
 - [2] L. Savary and L. Balents, *Reports on Progress in Physics* **80**, 016502 (2016).
 - [3] K. Kimura, S. Nakatsuji, J. Wen, C. Broholm, M. Stone, E. Nishibori, and H. Sawa, *Nature communications* **4**, 1934 (2013).
 - [4] J.-J. Wen, S. M. Koohpayeh, K. A. Ross, B. A. Trump, T. M. McQueen, K. Kimura, S. Nakatsuji, Y. Qiu, D. M. Pajerowski, J. R. D. Copley, and C. L. Broholm, *Phys. Rev. Lett.* **118**, 107206 (2017).
 - [5] J. S. Gardner, M. J. P. Gingras, and J. E. Greedan, *Rev. Mod. Phys.* **82**, 53 (2010).
 - [6] B. C. den Hertog and M. J. P. Gingras, *Phys. Rev. Lett.* **84**, 3430 (2000).
 - [7] R. G. Melko, B. C. den Hertog, and M. J. P. Gingras, *Phys. Rev. Lett.* **87**, 067203 (2001).
 - [8] S. T. Bramwell, M. J. Harris, B. C. den Hertog, M. J. P. Gingras, J. S. Gardner, D. F. McMorrow, A. R. Wildes, A. L. Cornelius, J. D. M. Champion, R. G. Melko, and T. Fennell, *Phys. Rev. Lett.* **87**, 047205 (2001).
 - [9] K. A. Ross, L. Savary, B. D. Gaulin, and L. Balents, *Phys. Rev. X* **1**, 021002 (2011).
 - [10] M. J. Gingras and P. A. McClarty, *Reports on Progress in Physics* **77**, 056501 (2014).
 - [11] S. Koohpayeh, D. Fort, and J. Abell, *Progress in Crystal Growth and Characterization of Materials* **54**, 121 (2008).
 - [12] S. Koohpayeh, J.-J. Wen, B. Trump, C. Broholm, and T. McQueen, *Journal of Crystal Growth* **402**, 291 (2014).
 - [13] N. Martin, P. Bonville, E. Lhotel, S. Guitteny, A. Wildes, C. Decorse, M. Ciomaga Hatnean, G. Balakrishnan, I. Mirebeau, and S. Petit, *Phys. Rev. X* **7**, 041028 (2017).
 - [14] N. Tang, A. Sakai, K. Kimura, S. Nakamura, M. Fu, Y. Matsumoto, T. Sakakibara, and S. Nakatsuji, *Proceedings of the International Conference on Strongly Correlated Electron Systems (SCES2019)*, 011090 (2020).
 - [15] A. S. Patri, M. Hosoi, S. B. Lee, and Y. B. Kim, *Phys. Rev. Research* **2**, 033015 (2020).
 - [16] E. Constable, R. Ballou, J. Robert, C. Decorse, J.-B. Brubach, P. Roy, E. Lhotel, L. Del-Rey, V. Simonet, S. Petit, and S. deBrion, *Phys. Rev. B* **95**, 020415(R) (2017).
 - [17] X. Zhang, Y. Luo, T. Halloran, J. Gaudet, H. Man, S. M. Koohpayeh, and N. P. Armitage, *Phys. Rev. B* **103**, L140403 (2021).

- [18] J. G. Rau and M. J. Gingras, Annual Review of Condensed Matter Physics **10**, 357 (2019).
- [19] P. Bonville, S. Guitteny, A. Gukasov, I. Mirebeau, S. Petit, C. Decorse, M. C. Hatnean, and G. Balakrishnan, Phys. Rev. B **94**, 134428 (2016).
- [20] Y. Xu and all, manuscript in preparation (2021).
- [21] A. J. Princep, D. Prabhakaran, A. T. Boothroyd, and D. T. Adroja, Phys. Rev. B **88**, 104421 (2013).
- [22] J. Gaudet, A. M. Hallas, C. R. C. Buhariwalla, G. Sala, M. B. Stone, M. Tachibana, K. Baroudi, R. J. Cava, and B. D. Gaulin, Phys. Rev. B **98**, 014419 (2018).
- [23] J. A. Sanjurjo, C. Rettori, S. Oseroff, and Z. Fisk, Phys. Rev. B **49**, 4391 (1994).
- [24] P. Thalmeier and P. Fulde, Phys. Rev. Lett. **49**, 1588 (1982).
- [25] S. W. Lovesey and U. Staub, Phys. Rev. B **61**, 9130 (2000).
- [26] M. Ruminy, S. Chi, S. Calder, and T. Fennell, Phys. Rev. B **95**, 060414(R) (2017).
- [27] P. Thalmeier, Journal of Applied Physics **55**, 1916 (1984).
- [28] E. Constable, R. Ballou, J. Robert, C. Decorse, J.-B. Brubach, P. Roy, E. Lhotel, L. Del-Rey, V. Simonet, S. Petit, and S. deBrion, Phys. Rev. B **95**, 020415 (2017).
- [29] For A_{1g} singlet level only vibronic interaction with a Γ -point phonon would produce a doublet.
- [30] B. A. Trump, S. M. Koohpayeh, K. J. Livi, J.-J. Wen, K. Arpino, Q. M. Ramasse, R. Brydson, M. Feygenson, H. Takeda, M. Takigawa, *et al.*, Nature communications **9**, 2619 (2018).